SUPPLEMENTAL MATERIAL

Supplemental Figures

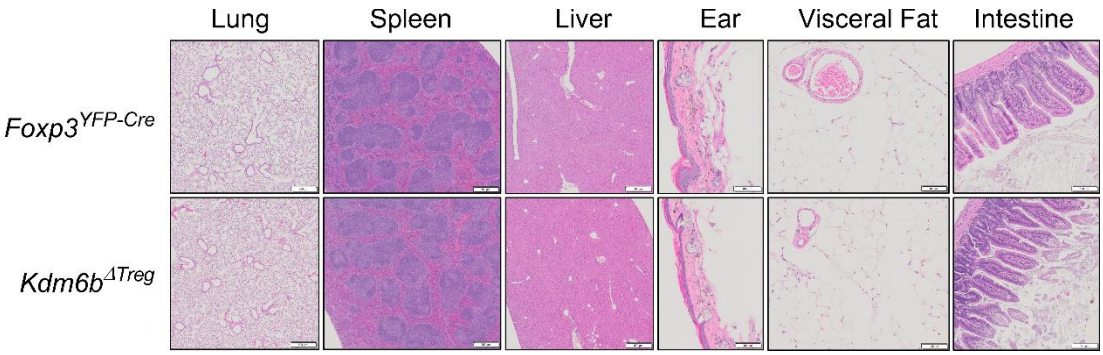

Supplemental Figure 1. Histological comparison of select organs from *Foxp3*$^{YFP\text{-}Cre}$ or *Kdm6b*$^{\Delta Treg}$ mice. Histological H&E section of organs from *Foxp3*$^{YFP\text{-}Cre}$ or *Kdm6b*$^{\Delta Treg}$ mice, aged 8-12 weeks. The white bar in the lung, spleen, and liver represents 500 μM, and the white bar in the ear, visceral fat, and intestine represents 100 μM. Sections from organs represent sections from *Foxp3*$^{YFP\text{-}Cre}$ or *Kdm6b*$^{\Delta Treg}$ mice (images representative of n = 3 – 4 mice per strain).

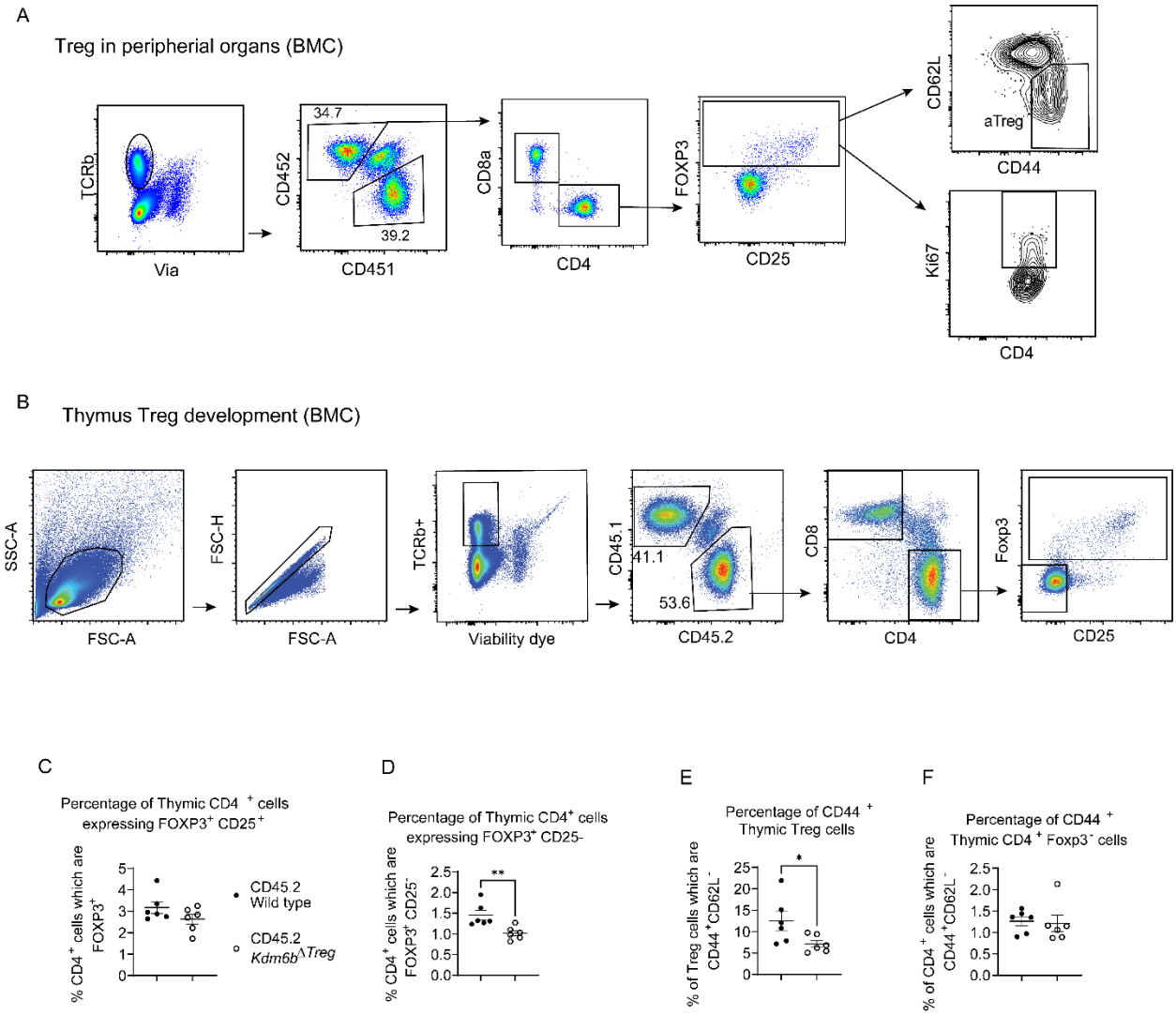

Supplemental Figure 2. Kdm6b regulates early thymic Treg activation status without altering overall Treg abundance.

(**A**) Representative flow cytometry gating strategy used to identify Tregs and activated/proliferating subsets in peripheral organs from mixed bone marrow chimeras (BMC). Immunophenotyping of $CD4^+FOXP3^+$ lymphocytes from splenocytes, lymph nodes (LN), or lung single-cell suspensions from a mixed bone marrow chimeric experiment after 8 weeks of engraftment comparing $CD45.2^+$ wild-type or $CD45.2^+$ *Kdm6b*$^{\Delta Treg}$ Tregs (n = 6 mice per condition).

(**B**) Gating strategy for analysis of thymic Treg development in BMC. (**C–D**) Quantification of the percentage of thymic $CD4^+$ T cells expressing $Foxp3^+$ $CD25^+$ (**C**) or $FOXP3^+$ $CD25^-$ (**D**) populations derived from WT ($CD45.2^+$) or *Kdm6b*$^{\Delta Treg}$ ($CD45.2^+$) donors in BMCs.

(**E**) Percentage of activated thymic Tregs ($CD44^+$ $CD62L^-$) among total $FOXP3^+$ Tregs. (**F**) Percentage of $CD44^+$ cells among thymic $CD4^+$ $FOXP3^-$ T cells. Data presented as mean ± SEM with p values derived from unpaired t-tests, * $p < 0.05$, ** $p < 0.01$

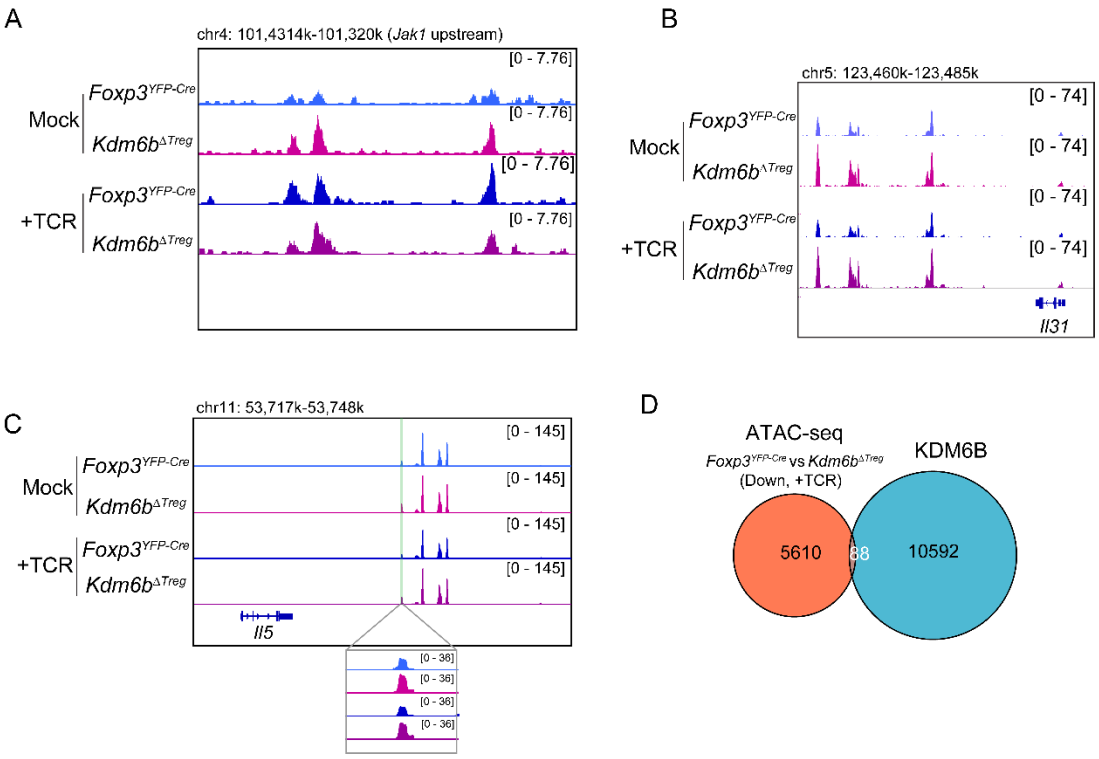

Supplemental Figure 3. Evaluation of chromatin accessibility at loci related to effector T cells.

TCR- vs mock-treated WT *Foxp3*$^{YFP\text{-}Cre}$ and *Kdm6b*$^{\Delta Treg}$ Tregs were subjected to ATAC-seq. Three replicates were combined for analysis. Normalized sequencing reads at the *Jak1* (**A**), *Il31* (**B**), and *Il5* (**C**) loci are shown. (**D**) Overlap between ATAC-seq peaks and Kdm6b ChIP-seq binding sites. Three replicates were combined for analysis.

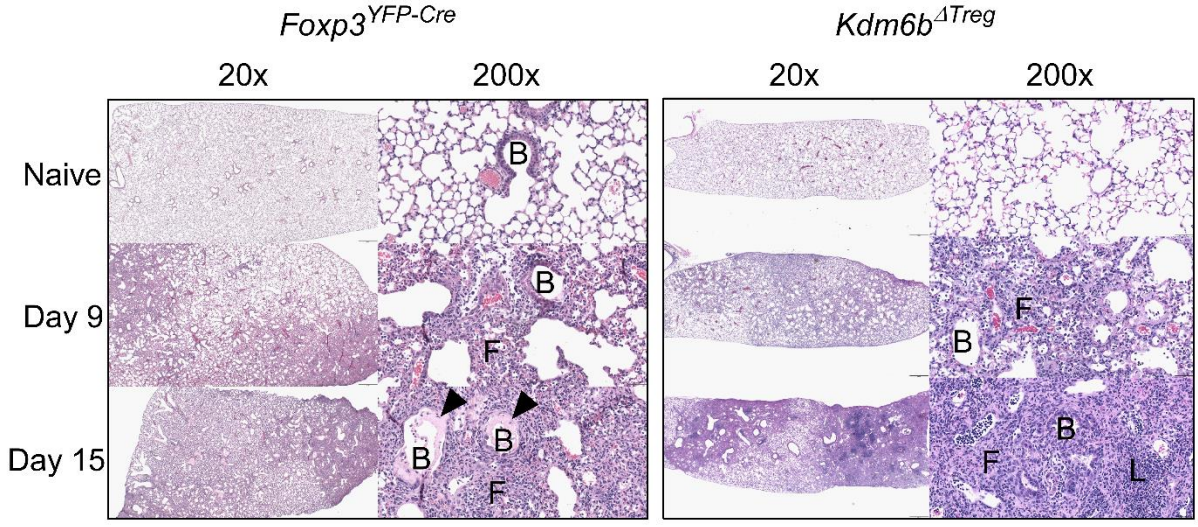

Supplemental Figure 4. Histological comparison of lung from *Foxp3*$^{YFP\text{-}Cre}$ or *Kdm6b*$^{\Delta Treg}$ mice. Histological H&E section of a lung from *Foxp3*$^{YFP\text{-}Cre}$ or *Kdm6b*$^{\Delta Treg}$ mice, aged 8-12 weeks at either naïve, day 9 or day 15 post PR8 infection. The black bar at 20x represents 500 μM and 50 μM at 200x. Sections are representative of lung findings from *Foxp3*$^{YFP\text{-}Cre}$ or *Kdm6b*$^{\Delta Treg}$ mice at each time point (at least 5 animals per group). *Foxp3*$^{YFP\text{-}Cre}$ or *Kdm6b*$^{\Delta Treg}$ mice administered influenza virus have a similar area of lung with bronchointerstitial pneumonia at Day 9 post infection, although the *Kdm6b*$^{\Delta Treg}$ mice did equivocally have more widespread inflammation than *Foxp3*$^{YFP\text{-}Cre}$ mice. Inflammation is comprised of neutrophils, macrophages, and lymphocytes with focally extensive areas of alveolar wall fibrosis, reorganizing fibrin, and bronchiolar epithelial cell degeneration, regeneration, and necrosis with bronchiolitis obliterans. At Day 15 post infection, the *Foxp3*$^{YFP\text{-}Cre}$ mice had less lung area with bronchointerstitial inflammation than the *Kdm6b*$^{\Delta Treg}$ mice. The nature of the inflammation was similar to Day 9, but the fibrosis and bronchiolar injury was more extensive. At Day 15, respiratory epithelial cell proliferation was present at a higher incidence and severity in the *Kdm6b*$^{\Delta Treg}$ group compared to the *Foxp3*$^{YFP\text{-}Cre}$ group. Additionally, lymphocytic aggregates were also evident at a higher incidence and severity in the *Kdm6b*$^{\Delta Treg}$ group compared to the *Foxp3*$^{YFP\text{-}Cre}$ group. Hyalinized rings (arrowhead; putatively denuded

bronchioles) were evident more frequently in the *Foxp3*$^{YFP\text{-}Cre}$ group than the *Kdm6b*$^{\Delta Treg}$ group. B=bronchiole; F=fibrosis; L=lymphocytic aggregates

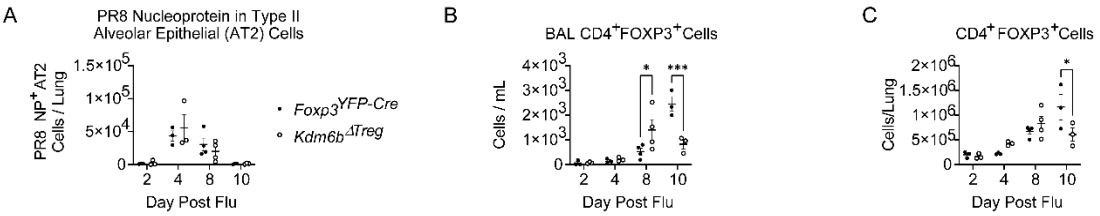

Supplemental Figure 5. Kinetics of PR8 viral infection and numbers of Tregs in the bronchoalveolar lavage and lung compartments.

Male and female *Foxp3*$^{YFP\text{-}Cre}$ and *Kdm6b*$^{\Delta Treg}$ mice 8 – 12 weeks of age were examined at either steady state or challenged with intratracheal Influenza A/PR/8/34 H1N1 (PR8) administered at day 0. Mice received 2 μL/g body weight for weight-based dosing as previously described (38). (**A**) Multicolor flow cytometry, as previously described, was used to determine the number of type II alveolar epithelial cells containing PR8 nucleoprotein antigen at several time points post PR8 infection in *Foxp3*$^{YFP\text{-}Cre}$ and *Kdm6b*$^{\Delta Treg}$ mice. (**B-C**) Tregs were enumerated from either bronchoalveolar lavage or lung single-cell suspensions at several time points post PR8 infection in *Foxp3*$^{YFP\text{-}Cre}$ and *Kdm6b*$^{\Delta Treg}$ mice (n = 3-4 mice per strain per time point). Data presented as mean ± SEM with p values derived from two-way ANOVA with Holm-Sidak multiple comparisons. * $p < 0.05$, *** $p < 0.001$.

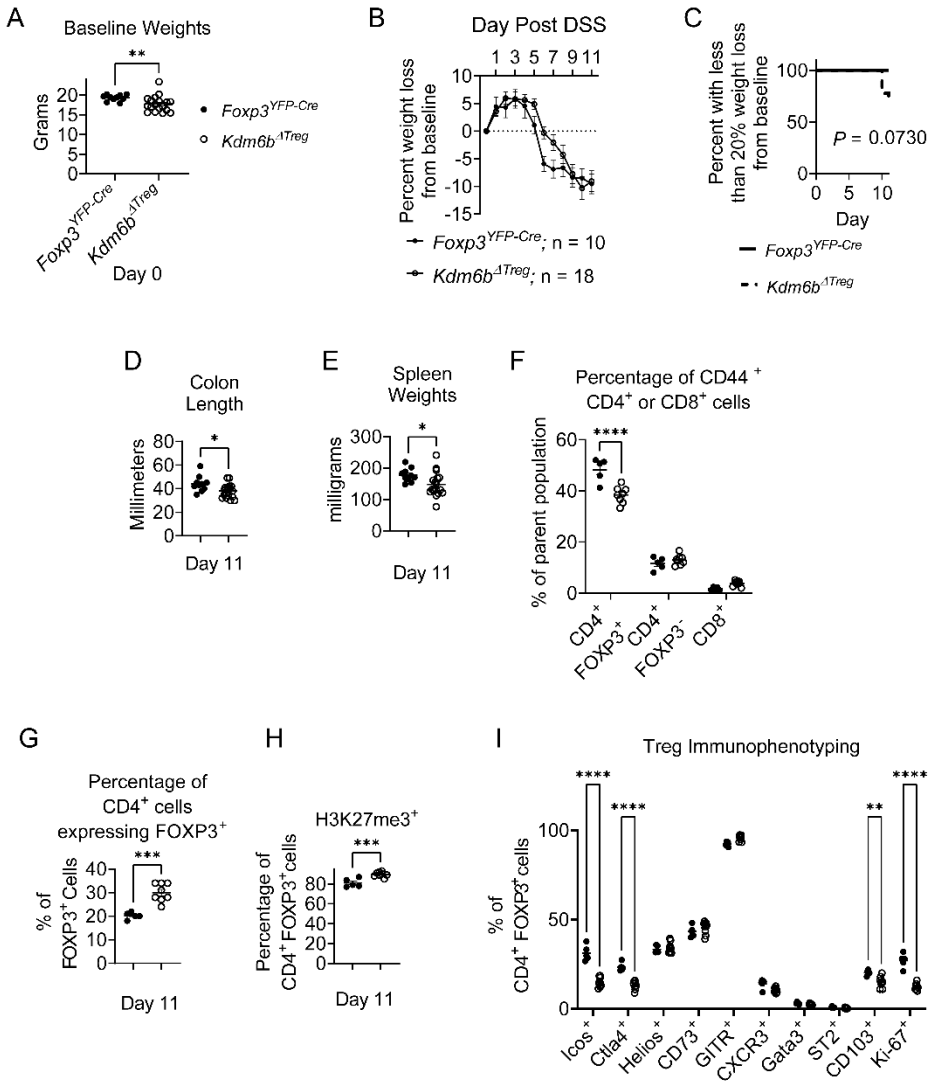

Supplemental Figure 6. Loss of *Kdm6b* in FOXP3⁺ Tregs exacerbates DSS colitis and alters Treg phenotype.

(**A**) Baseline body weights of female *Foxp3*$^{YFP\text{-}Cre}$ and *Kdm6b*$^{\Delta Treg}$ mice 8 – 12 weeks of age were examined at either steady state then challenged with 3% w/v of dextran sulfate sodium (DSS) in drinking water administered at day 0 as similar to previously described (54) (n = 10-18 mice per strain; combining 2 separate experiments).

(**B**) Percent weight loss from baseline over the DSS course in *Foxp3*$^{YFP\text{-}Cre}$ (closed circles) and *Kdm6b*$^{\Delta Treg}$ (open circles) mice.

(**C**) Proportion of mice maintaining ≥80% of baseline body weight over time following DSS initiation.

(**D**) Colon length and (**E**) spleen weights were measured at day 11.

(**F-I**) Immunophenotyping of mesenteric lymph nodes at day 11 (n = 5-8 per strain). (**F**) Frequencies of $CD44^+$ effector cells among $CD4^+$ and $CD8^+$ T cells. (**G**) Percentages of $CD4^+$ T cells expressing FOXP3 and (**H**) frequencies of $H3K27me3^+$ cells among $FOXP3^+$ $CD4^+$ T cells (**I**) Expression of canonical activation and lineage-defining markers (ICOS, CTLA4, Helios, CD103, GITR, CXCR3, GATA3, RORγt, CD103, Ki-67) on $FOXP3^+$ $CD4^+$ T cells assessed by flow cytometry. Data presented as mean ± SEM with p values derived from two-way ANOVA with Holm-Sidak multiple comparisons (**B**, **F**, **I**), unpaired t-test (**A**, **D**, **E**, **G**, **H**) and Log-Rank (**C**). * $p < 0.05$, ** $p < 0.01$, *** $p < 0.001$, **** $p < 0.0001$.

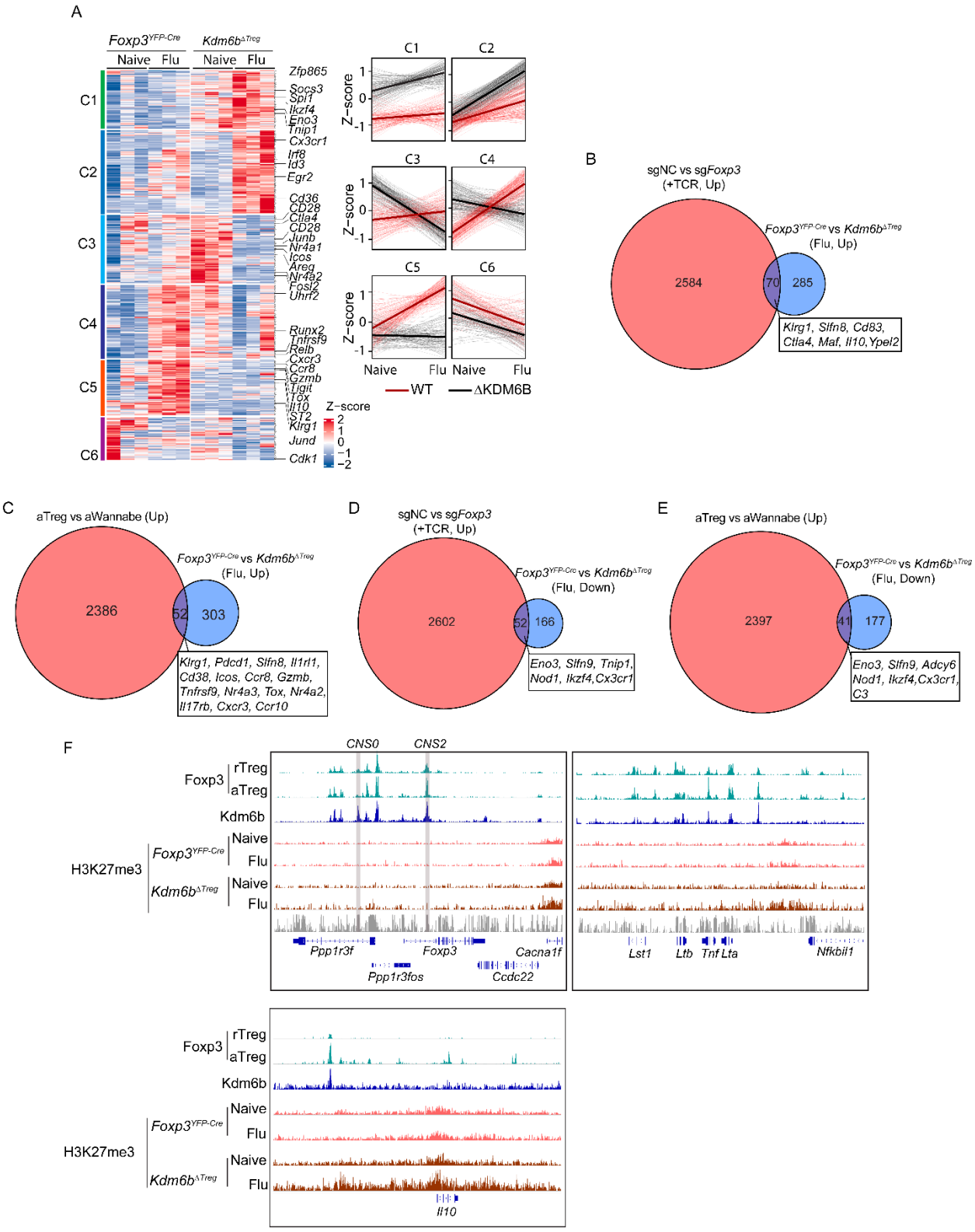

Supplemental Figure 7. KDM6B impact on lung Treg transcriptome at steady-state and during resolution of lung injury.

Male and female *Foxp3*$^{YFP\text{-}Cre}$ and *Kdm6b*$^{\Delta Treg}$ mice 8 – 12 weeks of age were examined at either steady state or challenged with intratracheal Influenza A/PR/8/34 H1N1 (PR8) administered at day 0. Mice received 2 μL/g body weight for weight-based dosing as previously described (38). Sorted lung Treg ($CD4^+YFP^+$) RNA from either *Foxp3*$^{YFP\text{-}Cre}$ or *Kdm6b*$^{\Delta Treg}$ mice at either steady-state or Day 15 post PR8 influenza were isolated, and RNA-seq was performed. Triplicates per condition.

(**A**) Gene expression patterns in lung Tregs from naive and flu virus-infected *Foxp3*$^{YFP\text{-}Cre}$ or *Kdm6b*$^{\Delta Treg}$ mice. Triplicates per condition.

(**B-E**) Number of genes regulated by FOXP3 (sgNC- versus sgFoxp3-transduced Tregs) (He et al., 2024), or aTreg versus activated Treg wannabe cells (aWannabe) (van der Veeken et al., 2020), and KDM6B in Tregs isolated from flu virus-infected lung.

(**F**) FOXP3, KDM6B, or H3K27me3 peaks at *Foxp3*, *Tnf*, or *IL10* gene regions. FOXP3 or KDM6B CUT&RUN showing binding in aTreg and rTreg cells was overlaid with separate CUT&RUN data showing H3K27me3 modification tracks from sorted in lung Tregs from naive and flu virus-infected *Foxp3*$^{YFP\text{-}Cre}$ or *Kdm6b*$^{\Delta Treg}$ mice. Triplicates per condition.

Supplemental Table S10

REAGENT or RESOURCE	SOURCE	IDENTIFIER
Antibodies		
CD194 (CCR4) anti-mouse - PE/Cy7 (clone: 2G12)	Biolegend	cat# 131214; RRID: AB_2244410
CD103 anti-mouse - BV605 (clone: 2E7)	Biolegend	cat# 121433; RRID: AB_2629724
CD103 anti-mouse - BV785 (clone: 2E7)	Biolegend	cat# 121439; RRID: AB_2800588
CD103 anti-mouse - PE/Cy7 (clone: 2E7)	Biolegend	cat# 121426; RRID: AB_2563691
CD19 anti-mouse - BV605 (clone: 6D5)	Biolegend	cat# 115540; RRID: AB_2563067
CD25 anti-mouse - APC/Cy7 (clone: PC61)	Biolegend	cat# 102026; RRID: AB_830745
CD3 anti-mouse - FITC (clone: 17A2)	Biolegend	cat# 100204; RRID: AB_312661
CD4 anti-mouse - Alexa 700 (clone: GK1.5)	Biolegend	cat# 100430; RRID: AB_493699
CD4 anti-mouse - BV786 (clone: RM4-5)	BD Biosciences	cat# 563727; RRID: AB_2728707
CD44 anti-mouse - BV510 (clone: IM7)	BD Biosciences	cat# 563114; RRID: AB_2738011
CD45 anti-mouse - BV785 (clone: 30-F11)	Biolegend	cat# 103149; RRID: AB_2564590
CD45 anti-mouse - FITC (clone: 30-F11)	Biolegend	cat# 103108; RRID: AB_312973
CD45.2 anti-mouse - PE (clone: 104)	Biolegend	cat# 109808; RRID: AB_313445
CD45.2 anti-mouse - PE/Dazzle (clone: 104)	Biolegend	cat# 109846: RRID: AB_2564177
CD62L anti-mouse - BV650 (clone: MEL-14)	BD Biosciences	cat# 564108; RRID: AB_2738597
CD8α anti-mouse - Alexa 700 (clone: 53-6.7)	Biolegend	cat# 100730; RRID: AB_493703
CD8α anti-mouse - PE/Dazzle 594 (clone: 53-6.7)	Biolegend	cat# 100762; RRID: AB_2564027
Foxp3 anti-mouse - APC (clone: FJK-16s)	Invitrogen	cat# 17-5773-82; RRID: AB_469457
Helios anti-mouse/human - FITC (clone: 22F6)	Biolegend	cat# 137214; RRID: AB_10662745
I-A/I-E (MCH II) anti-mouse - Alexa 700 (clone: M5/114.15.2)	Biolegend	cat# 107622; RRID: AB_493727
IFN-γ anti-mouse - BV510 (clone: XMG1.2)	Biolegend	cat# 505841; RRID: AB_2562187
Influenza A NP Monoclonal-FITC (clone: D67J)	Invitrogen	cat# MA1-7322; RRID: AB_1017747
Ki-67 anti-mouse - BV421 (clone: 16A8)	Biolegend	cat# 652411; RRID: AB_2562663
Ki-67 Monoclonal -PE (clone: SolA15)	Invitrogen	cat# 12-5698-82; RRID: AB_11150954
KLRG1 (MAFA) anti-mouse/human - BV605 (clone: 2F1/KLRG1)	Biolegend	cat# 138419; RRID: AB_2563357
TCR γ/δ anti-mouse - PerCP/Cy 5.5 (clone: GL3)	Biolegend	cat# 118118; RRID: AB_10612756
TNFα anti-mouse - PerCP/Cy5.5 (clone: MP6-XT22)	Biolegend	cat# 506322; RRID: AB_961434
Tri-Methyl-Histone H3 (Lys27) - PE (clone: C36B11)	Cell Signaling Technology	cat# 40724S
Tri-Methyl-Histone H3 (Lys27)	Cell Signaling Technology	cat# 9733S

Anti-KDM6B / JMJD3 antibody	Abcam	Cat# ab38113
Zombie Aqua Fixable Viability Kit	Biolegend	cat# 423102
Zombie NIR Fixable Viability Kit	Biolegend	cat# 423106
Chemicals, peptides, and recombinant proteins		
Biolegend cell activation cocktail	Biolegend	Cat# 423304
RPMI-1640 medium	GIBCO, Life Technologies	Cat# 52400-025
Collagenase, type I	Worthington Biochemicals	Cat# LS004197
CFSE	BD Bioscience	Cat# 565082
DNAse	Worthington Biochemicals	Cat# LS002139
Human IL2	ThermoFisher, Peprotech	Cat# 200-02
Dextran Sulfate Sodium Salt	ThermoFisher,	Cat# J63606.22
Neomycin	Millipore Sigma	Cat# 1458019
Miltenyi CD3/CD28 Bead Kit	Miltenyi	Cat# 130-093-627
Hot Start High-Fidelity DNA Polymerase	New England Biolabs	Cat# M0515S
pAG-MNase	He *et al.*[29]	N/A
Digitonin	Millipore	Cat# 300410-1GM
KAPA Hyper prep kit	Kapa Biosystems	Cat# KK8504
SPRIselect	Beckman Coulter	Cat# B23318
EDTA (0.5 M), pH 8.0, RNase-free	Invitrogen	Cat# AM9261
Low melting agarose	Invitrogen	Cat# 16520100
EGTA	Sigma-Aldrich	Cat# 3889
Percoll	Sigma-Aldrich	Cat# GE17-0891-01
TRIzol RNA isolation reagents	Thermo Fisher Scientific	Cat# 10296010
Mouse T-Activator CD3/CD28 beads	Thermo Fisher Scientific	Cat# 11456D
Foxp3 / transcription factor staining buffer set	eBioscience	Cat# 00-5523-00
Spermidine	Sigma-Aldrich	Cat# S2626
Influenza A/PR/8/34 H1N1 (PR8)	Charles River	Cat# 10100374
Critical commercial assays		
EasySep Mouse CD4+CD25+ Regulatory T Cell Isolation Kit II	StemCell Technologies	Cat# 18783
CUT&RUN Assay Kit	Cell Signaling Technologies	Cat# 86652
KAPA Mouse Genotyping Kits - HotStart PCR	Fisher Scientific	Cat# 50-196-5243
Quick-RNA MicroPrep Kit, Zymo Research	Fisher Scientific	Cat# 50-444-592
NucleoSpin Gel and PCR Clean-up Mini Kit	Macherey-Nagel	Cat# 740609.50
Qiagen MinElute PCR Purification Kit	Qiagen	Cat# 28006
DNA Purification Buffer and Spin Column Kit	Cell Signaling Technologies	Cat# 14209
BSA Protein Assay	Bio-Rad Laboratories	Protein Assay Reagent A: 5000113 Protein Assay Reagent B: 5000114 Quick Start BSA Standard 2mg/ml: 5000206
Oligonucleotides		
Kdm6b primers	Sigma	Jmjd3-F: CAGAGGCAGGTAGATCTTTG Jmjd3-F3: GAGGTGAAGAACGTCAAGTC Jmjd3-R: CAACCCTCCCTTTCTTTTCG
Foxp3 Cre primers	Sigma	forward: AGGATGTGAGGGACTACCTCCTGTA reverse: TCCTTCACTCTGATTCTGGCAATTT
Foxp3 Cre Wildtype primers	Sigma	forward: CCTAGCCCCTAGTTCCAACC reverse: AAGGTTCCAGTGCTGTTGCT
Other		
Plasmid pSIR-BbsI-Thy1.1	Li et al. [31]	